Available online at www.sciencedirect.com

ScienceDirect

Procedia Manufacturing 11 (2017) 1667 – 1674

Procedia MANUFACTURING

27th International Conference on Flexible Automation and Intelligent Manufacturing, FAIM2017, 27-30 June 2017, Modena, Italy

Automatic features recognition for anthropometry

Di Angelo L.*, Di Stefano P., Pane C.

Department of Industrial and Information Engineering, and of Economics - University of L'Aquila, via G. Gronchi 18, 67100 L'Aquila, Italy

Abstract

For the purpose of reducing uncertainties in the measurements of morphologically complex biological objects, the authors present a new automatic method, which takes advantage from the representation of the object in the form of the 3D geometric model obtained from CT-scans or 3D scanning. In this paper, the method is verified in real cases and compared with the traditional approaches.

Peer-review under responsibility of the scientific committee of the 27th International Conference on Flexible Automation and Intelligent Manufacturing

Keywords: 3D biomedical image analysis; measurement protocols in biomedicine; measurement accuracy; shape segmentation.

1. Introduction and related works

The biological objects are morphologically complex elements, which perform a particular physiological function. In many applications, geometric and dimensional parameters of these components of the human body are analyzed to gather some evidence, which may be useful in medicine, anthropology and forensic investigations. In latest related literature, measures of human bones are analyzed for:

- monitoring physiological events [1][2];
- assess dental shapes to improve orthodontic treatment planning [2];
- evaluation of susceptibility to diseases [3];

* Corresponding author. Tel.: +39 0862434310;
E-mail address: luca.diangelo@univaq.it

Peer-review under responsibility of the scientific committee of the 27th International Conference on Flexible Automation and Intelligent Manufacturing
doi:10.1016/j.promfg.2017.07.290

- body mass estimation ([4], [5] and [6]);
- identification of the height, posture and locomotion mode of a subject ([6], [7] and [7]) or of a specific anatomical part [9]), gender, age and ethnicity of the subject ([10] and [11]).

In each of the previously described applications, measures are required to be accurate enough to discriminate the factor being investigated. Generally speaking, the measurements are performed in-vitro or in-vivo. In the first case, manual measuring devices, such as sliding caliper and a goniometer are used. In-vivo, when the component of the human body is available in the form of a 3D geometric model (as it is the case of CT-scans or X-ray images) [12], its measurement is performed as the point-to-point distance between points manually selected by the operator in a specific software. All these approaches are not structured since the measure is not associated with an ideal feature, as prescribed by GPS standards. It is mainly for this reason that this kind of measures is affected by wide uncertainties.

With the aims to reduce the measurement uncertainties, the authors presented a new automatic methodology to measure morphologically complex objects, which takes advantage from the representation of the object as a 3D geometric model obtained from CT-scans or 3D scanning. In this paper, the method is verified in real cases and compared with the traditional approaches.

2. Measurement protocols in biomedicine

Each time an element has to be dimensionally characterized, it is fundamental to follow an approved measurement protocol. Indeed, only in this way, it is possible to predict the reproducibility and repeatability of the process or the accuracy of the measurement itself. In other words, only in this case, it is possible to compare measurements performed at different times, by different operators, in different laboratories. This problem has been addressed by GPS standards, for the sculptured surface, whose shape can be typically approximated by an analytical surface (plane, cylinder, cone, etc.). By the recognition of some features (nominal features, integral features, derived features, etc), and some operations (partition, extraction, association), the GPS standards define rigorously measurement protocols for both manual and automatic devices. That cannot occur in the field of biomedicine since objects to be measured are morphologically complex; so that, it is not possible to associate an ideal feature as prescribed by GPS standards.

The definition of measurement protocols for the dimensional characterization of human bones always refers to the use of manual devices (manual caliper, goniometer). Furthermore, for their complex morphology is not possible to define certain references based on them. This gives rise to a lack of standard protocols, which often provide rough indications. This determines that the expert operator must visually segment the part to be measured and, based on his experience, interpret and apply the measurement rules.

By way of example, the figures 1 and 2 show, respectively, the measuring features and the corresponding measurements protocols for the most important dimensional features of thoracic and lumbar vertebrae (MP_V in figure 1) and maxillary incisor (MP_T in figure 2). Both the measuring protocols refer to a local reference system of the object. In the MP_v, the measures of the body, spinous process, and the vertebral canal are performed in the *sagittal* and *traverse* planes. In the case of maxillary incisors, the tooth the dimensional characterization of crown and root are performed in the *labial* and *proximal* views. Neither protocol provides precise guidelines on how to build the system of reference and segmenting the object in implementing the measures. These lacks in protocols necessarily require interpretation by the operator and this results in a poor accuracy of the measurements.

3. The computer-aided measurement methodology

Figure 3 shows the flow-chart of the proposed methodology. The first four steps are necessary to set up the geometric model to be submitted to the automatic measurement methodology. Even if they require the interaction of an operator, these phases are coded and are consequently easily reproducible and repeatable.

Once a valid geometric model is available, the proposed methodology performs the dimensional feature measurements in an algorithmic way (without any interaction with the operator), according to the following three phases:

- Local reference system definition;

- Derived geometric features recognition;
- Dimensional features evaluation.

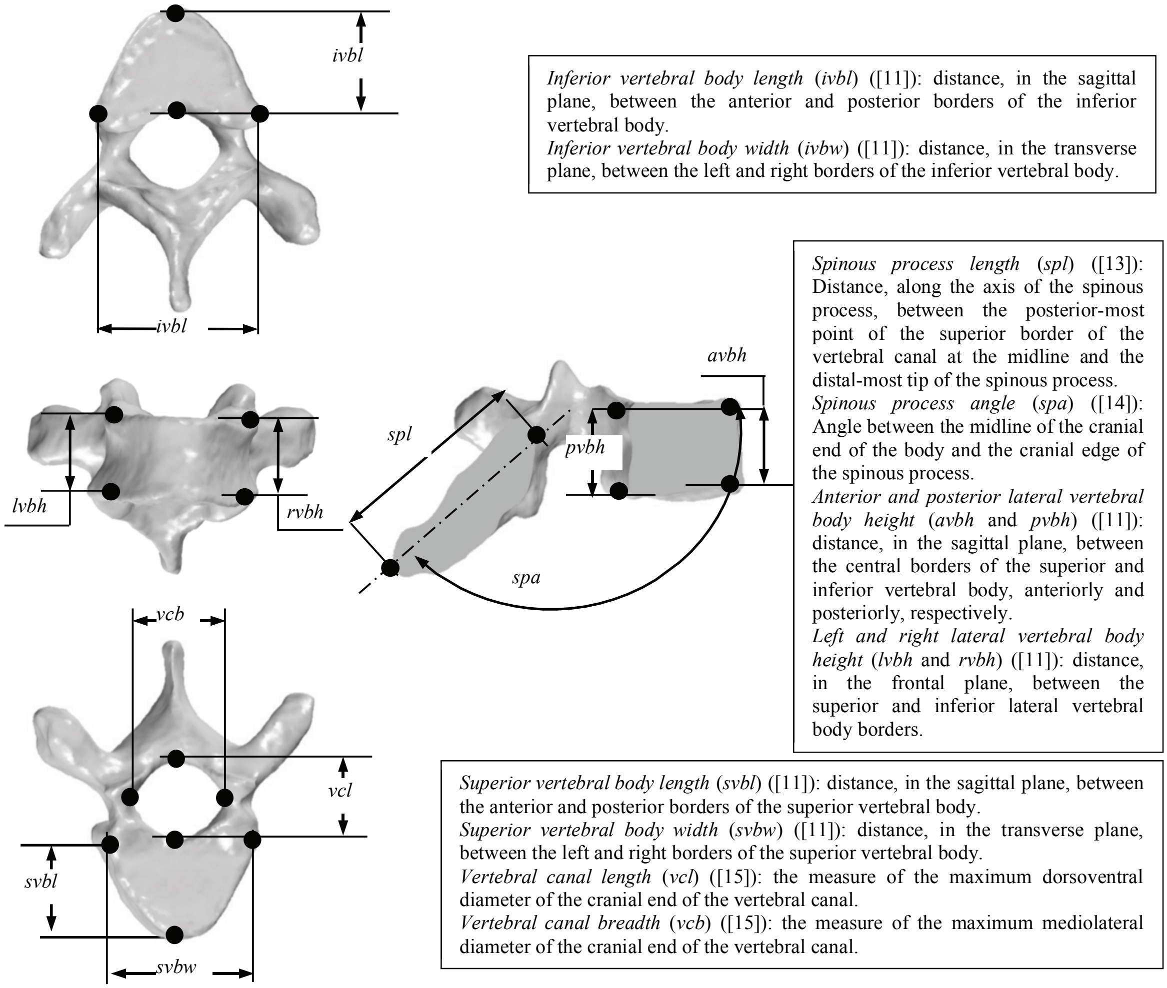

Figure 1. The measuring features with the corresponding measurements protocol of the vertebra (*MP_V*)

In order to implement each of these phases, the methodology codifies, in mathematical and geometric expressions, the guidelines deducted from the measurement protocols.

The proposed automatic methodology, firstly, identifies the Local Reference System (LRS) of the model. With the aim to identify in a repeatable way the *LRS*, a robust protocol must be defined. At this purpose, the methodology analyses specific geometric and morphological evidence detectable on 3d geometric models to implement, algorithmically, the recommendations of PMv and PM_T. The two cases analyzed (vertebrae and tooth) are morphologically so different to require two different algorithms.

Regarding the vertebrae, the *LRS* are based on the following features (figure 4):

- The *symmetry plane* Π_S of the vertebra;
- The *vertebral cylinder* Ω, which is the analytical cylinder approximating the vertebral foramen *VF*;
- The *coronal plane* Π_c, which divides the vertebra into the body and the posterior element;
- The *middle plane* Π_M of the vertebra's body;

- The *second coronal plane* Π_B, which divides the vertebra's body;
- The *axis of the posterior spinous process* $\mathbf{a}_s$.

More details about the rules to identify each of the previously reported features and to segment the vertebra are reported in [17].

The measurement protocol consists of the following steps:

- The tooth is placed along its longitudinal axis in a dental surveyor with a red wax support;
- The maximum crown contour or anatomic equator (E) is drawn on the tooth's crown with a graphic pencil;
- On its labial side, the most apical point of the cement–enamel junction (CEJ) is marked as Point 1;
- The most apical points of the anatomic equator are marked as Point 2 on the labial surface, and Point 3 on the lingual surface;
- The most basal points of the equator on the mesial and distal surfaces are marked as Points 4 and 5, respectively;
- A line surrounding the whole root is drawn 3mm from Point 1. Points 6 and 7 are on this line in the middle of labial and lingual surfaces.

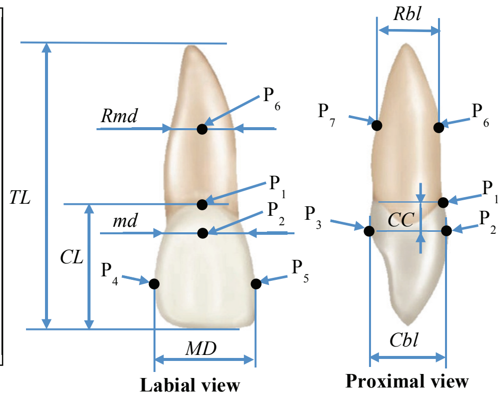

The following dimensional features are identified:

- *Crown length* (*CL*): defined as the distance between the Point 1 and the incisal edge of the crown;
- *Total length* (*TL*): defined as *CL* plus root length to the apex;
- *Cervical axial diameter* or *cervical convexity* (*CC*): measured from Point 1 to Point 2;
- *Major mesio-distal diameter* (*MD*): from mesial Point 3 to distal Point 4;
- *Minor mesio-distal diameter* (*md*): parallel to *MD* at labial Point 2;
- *Root mesio-distal diameter* (*Rmd*): parallel to MD at Points 6–7 height;
- *Crown buccolingual diameter* (*Cbl*): from labial Point 2 to lingual Point 3;
- *Root buccolingual diameter* (*Rbl*): from root labial Point 6 to root lingual Point 7.

Figure 2. The measuring features with the corresponding measurements protocol of the maxillary central incisor (MP_T)

The reference frame of the tooth consists of three mutually orthogonal planes (*mesiodistal* Π_M, *labiolingual* Π_L and *transversal* Π_T), as shown in figure 5. The algorithm introduced in this paper identifies these planes by evaluating the *Principal Component* of inertia of the tooth. The *labial side* of the tooth is distinguished from the *lingual* one by analyzing the curvature of the sectioning curve obtained by the intersection of the tooth with the *labiolingual plane* (Π_L). More details are reported in [18].

Once the geometric model is aligned to the *LRS*, the proposed methodology, algorithmically, recognizes the derived geometric features recognition and evaluates dimensional features. The figures 6 and 7 report the proposed rules, respectively, for MCI and for thoracic and lumbar vertebrae. In both cases, the dimensional features are grouped together according to the characteristics plane on which are identified.

4. Results and conclusion

In order to compare the measurements accuracy performed with the manual methods (*MM*) by following the protocols of figures 1 and 2 with those of the presented *computer-based method* (CBM), a specific experimentation is carried out. The principal characteristics are summarized in table 1. Since any measurement uncertainties in the dimensional features result from the contribution of both *intra-tester repeatability* and *inter-tester reproducibility*, in this paper these two components of measurement error are analyzed.

In order to evaluate the *Intra-tester repeatability* (*TRA*), each of the 12 testers has performed 20 measures for each dimensional feature of vertebrae and the tooth, under repeatability experimental conditions. Regarding the *CBM*, each of 12 testers scanned 20 times the same models. The *TRA* is evaluated as the standard deviations of the performed measurements.

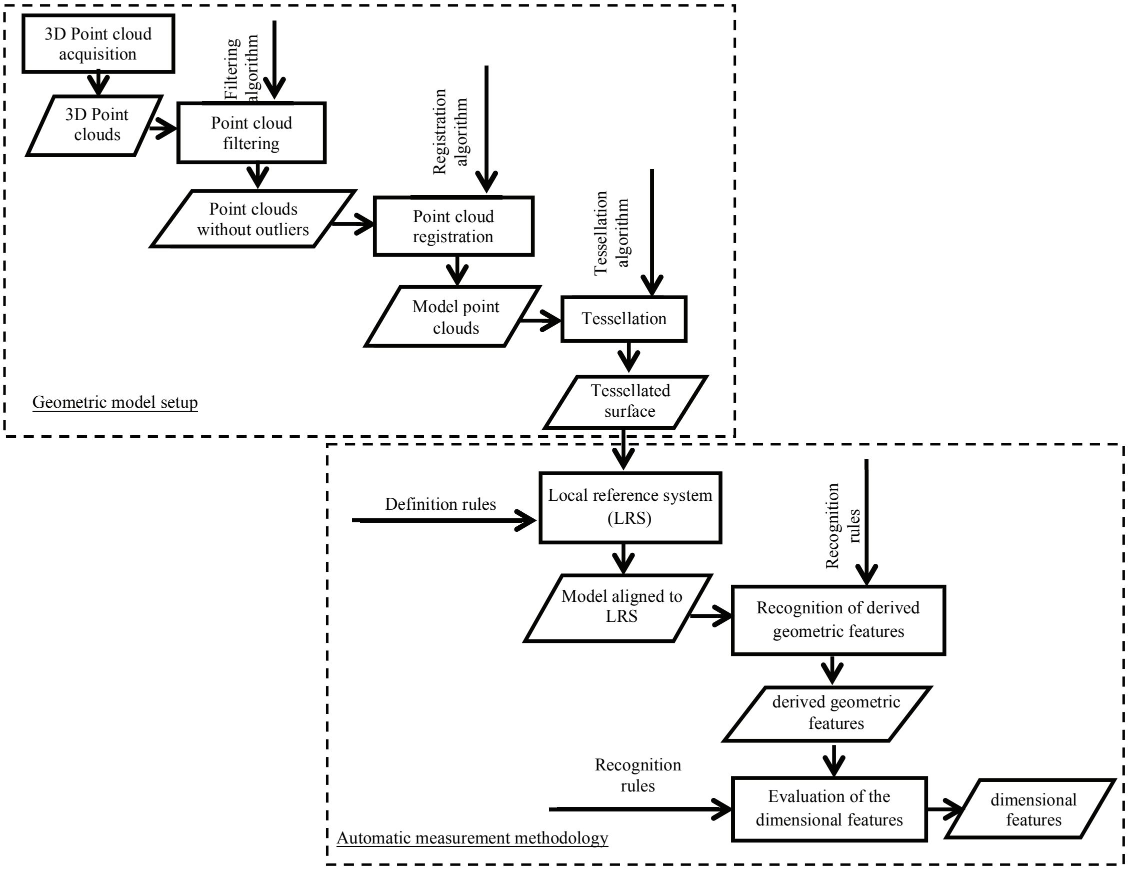

Figure 3. The flow-chart of the proposed methodology

Table 1. –Experimental conditions to characterize the accuracy of measurements performed by MP_V and MP_T.

	MP_V	MP_T
Testers	12 medical students in the fifth year of their medical course and onwards, trained appropriately. All the testers have been blinded to the results of the measurements	
Materials	A thoracic (*TV*) and a lumbar vertebra (*LV*) randomly selected by a set of 10 vertebrae (5 thoracic and 5 lumbar) of different adults over 18 years of age. All the vertebrae have a normal morphology and are clean, without evidence of diseases.	A tooth randomly selected by a set of 20 incisors extracted from adults over 18 years of age. All the teeth have a normal morphology and are clean, free of restorations and decay, and without excessive evidence of incisal wear.
Measurement devices for MM	Sliding caliper and goniometer	Dental surveyor and Sliding caliper
Measurement device for CBM	calibrated FARO® Edge, 9 ft (2.7m) laser scanner (point repeatability 0.024 mm - 0.064 mm and the average point spacing 0.1 mm)	
Test of normality	Kolmogorov-Smirnov	

The tables 2 and 3 report, respectively, the results for MP_V (table 2) and for MP_T (table 3), implemented by *MM* and *CBM*.

The repeatability of traditional methods in the dimensional features depends on the intrinsic complexity to measure some dimensional features and, in many cases, does not permit to discriminate the factor being investigated. Regarding the *CBM*, since the parameters are calculated algorithmically, the *Intra-tester repeatability* is affected mainly by the point cloud registration process, rate sample of the model and the measuring noise. The repeatability of the *CBM* is, in any of the tested cases, greater than that observed in *MM* and its order of magnitude is such as to allow a discrimination of the factor being investigated.

The degree of reproducibility reached through the proposed method is higher than that shown through the other method for all the dimensional features: it is on average 6 times lower than with the *MM*, both for teeth that for the vertebrae. In order to quantify this difference in terms of *TER*, we consider the variations of the *spa* angle for TV and *ratio md/MD* for teeth. In the first case, the extreme mean values measured by the operators vary from 109° to 134° for *MM*, and from 108.3 to 108.5 for *CBM*. The variation for *MM* is so great that different operators can identify, based on this angle, a different type of vertebra [16]. The same considerations are valid for *TER* measured for a tooth. At varying the operator measuring the tooth, the range of variation of the *ratio md/MD* is such that the same tooth is attributed, by different testers, at a different morphology category [3].

Since any measurement uncertainties in the dimensional features result from the contribution of both *intra-tester repeatability* and *inter-tester reproducibility*, the carried out experimentation shows that the proposed methodology is more accurate than the state-of-the-art. The high accuracy of the method and the objective measures, which it provided, may open up the road to new investigations in anthropology.

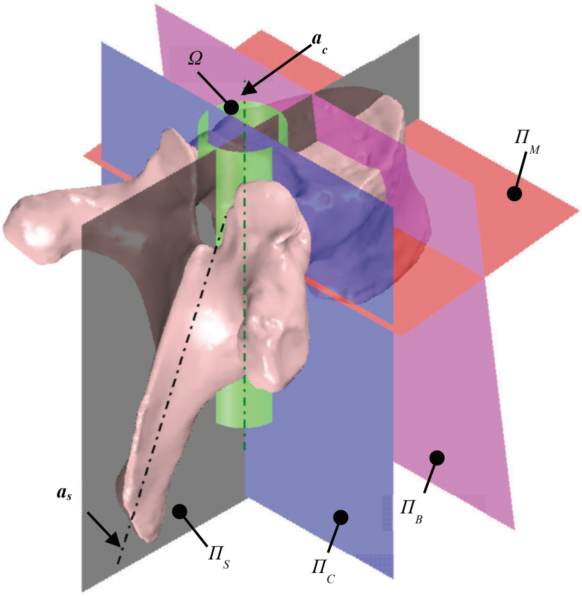

Figure 4. The LRS elements definition for the vertebra.

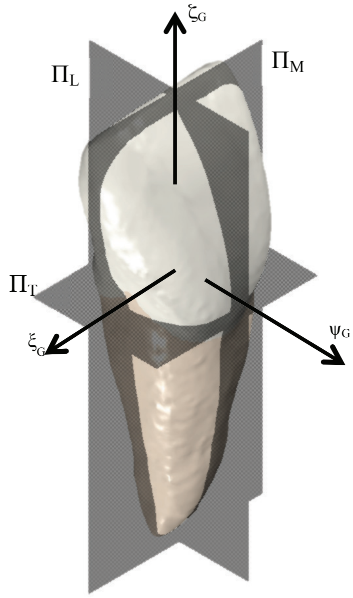

Figure 5. The LRS elements definition for the tooth.

References

[1]. Kolta, S., Kerkeni, S., Travert, C., Skalli, W., Eastell, R., Glüer, C.C., Roux, C., 2012. Variations in vertebral body dimensions in women measured by 3D-XA: a longitudinal in vivo study. Bone 50(3), 777–783.

[2]. S. Barone, A. Paoli, A.V. Razionale, CT segmentation of dental shapes by anatomy-driven reformation imaging and B-spline modeling, International Journal for Numerical Methods in Biomedical Engineering, 32 (2016) 1-17

[3]. Lazos JP, Senn LF, Brunotto MN. Characterization of maxillary central incisor: novel crown-root relationships. Clin Oral Investig. 2014; 18: 1561–1567.

[4]. Squyres, Nicole, and Christopher B. Ruff. "Body mass estimation from knee breadth, with application to early hominins." American journal of physical anthropology 158.2 (2015): 198-208.

[5]. Sládek, Vladimír, et al. "Body mass estimation in skeletal samples using the hybrid approach: the effect of population-specific variations and sexual dimorphism." Archaeological and Anthropological Sciences (2016): 1-15.

[6]. White T.D., M. Black, T., Folkens, P.A., 2000. Human Osteology, second ed., Academic Press, San Diego.

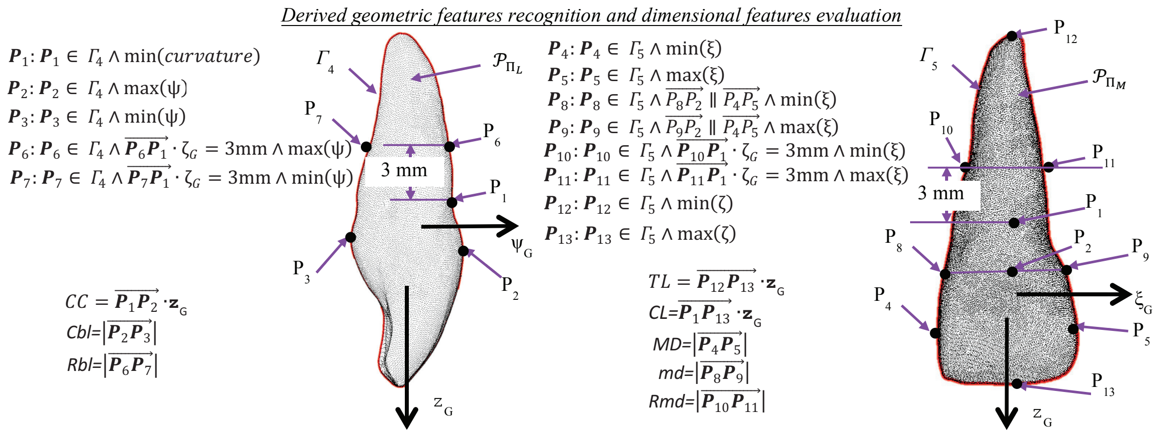

Figure 6. The derived geometric features recognition and dimensional features evaluation for MCI.

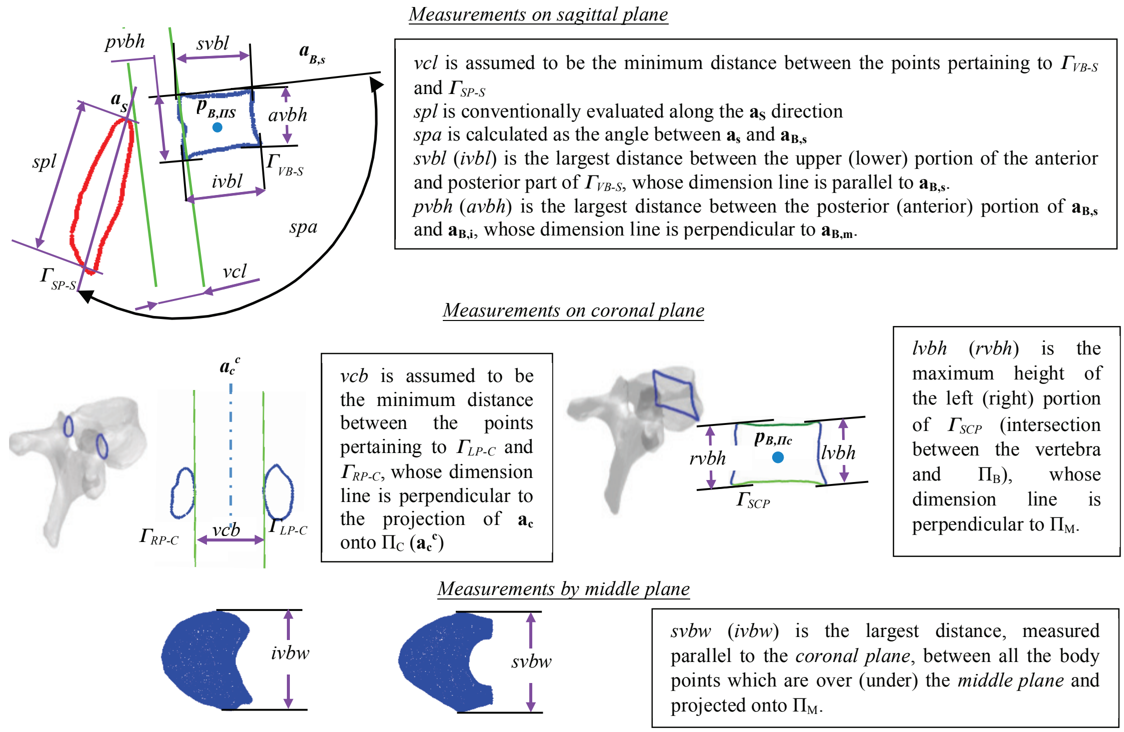

Figure 7. The derived geometric features recognition and dimensional features evaluation for thoracic and lumbar vertebrae

[7]. Reiss, Stefan, and Heinrich Mallison. "Motion range of the manus of Plateosaurus engelhardti von Meyer, 1837." Palaeontologia Electronica 17.1 (2014): 1-19.
[8]. Furferi, R., Governi, L., Uccheddu, F., & Volpe, Y. (2017). A RGB-D based instant body-scanning solution for compact box installation. In Advances on Mechanics, Design Engineering and Manufacturing (pp. 819-828). Springer International Publishing.
[9]. Baronio G., Harran S., and Signoroni A. (2016). A Critical Analysis of a Hand Orthosis Reverse Engineering and 3D Printing Process. Applied Bionics and Biomechanics, 2016.
[10].Masharawi, Y., Salame, K., 2011. Shape variation of the neural arch in the thoracic and lumbar spine: characterization and relationship with the vertebral body shape. Clin Anat 24, 858–867.
[11].Zheng, W.X., Cheng, F.B., Cheng, K.L., Tian, Y., Lai, Y., Zhang, W.S., Zheng, Y.J., Li Y.Q., 2012. Sex assessment using measurements of the first lumbar vertebra. Forensic Science International 219, 285.e1–285.e5.

[12].Filippi S, Motyl B, Bandera C. Comparing parametric solid modelling/reconfiguration, global shape modelling and free-form deformation for the generation of 3D digital models of femurs from X-ray images. Computer Methods in Biomechanics and Biomedical Engineering, (2009), 12 (1), pp. 101-108
[13].O'Higgins, P., Milne, N., Johnson, D.R., Runnion, C.K., Oxnard, C.E., 1997. Adaptation in the vertebral column: A comparative study of patterns of metameric variation in mice and men. Journal of Anatomy 190, 105–113.
[14].Latimer, B., Ward, C. V., 1993. The thoracic and lumbar vertebrae. In: A. Walker and R. Leakey (Eds.) The Nariokotome Homo erectus skeleton. Cambridge, MA: Harvard Univ. Press, pp. 266–293.
[15].Martin, R., 1928. Lehrbuch der Anthropologie in Systematischer Darstellung mit Besonderer Berücksichtigung der anthropologischen Methoden für Studierende, Ärtze und Forschungsreisende, vol. 2: Kraniologie, Osteologie. Jena, Germany: Gustav Fischer. pp 345-355.
[16].Singh, R., Srivastva, S. K., Prasath, C. S. V., Rohilla, R. K., Siwach, R., & Magu, N. K. (2011). Morphometric measurements of cadaveric thoracic spine in Indian population and its clinical applications. Asian spine journal, 5(1), 20-34.
[17].Di Angelo L., Di Stefano P., "A new method for the automatic identification of the dimensional features of vertebrae". Computer Methods and Programs in Biomedicine, vol. 121 (1), 2015, pp. 36-48.
[18].Di Angelo L., Di Stefano P., Bernardi S., Continenza M.A., "A new computational method for automatic dental measurement: The case of maxillary central incisor". Computers in Biology and Medicine, vol. 70, 2016, pp. 202-206.

Table 2. –Comparison of *intra-tester repeatability* and the *inter-tester reproducibility* of MP_V implemented by by *TD* and *CATM*.

	dimensional parameter	*TV*				*LV*			
		TRA		*TER*		*TRA*		*TER*	
		MM	*CBM*	*MM*	*CBM*	*MM*	*CBM*	*MM*	*CBM*
spinous process	*spl*	0.41	0.11	0.46	0.20	0.59	0.07	2.02	0.24
	spa	7.63	0.17	8.30	0.18	7.10	0.15	13.71	0.32
body	*svbl*	0.24	0.05	0.21	0.14	0.36	0.08	0.41	0.18
	svbw	0.38	0.10	1.35	0.10	0.31	0.05	0.35	0.20
	ivbl	0.23	0.20	0.13	0.07	0.22	0.21	0.10	0.11
	ivbw	0.38	0.08	0.47	0.08	0.25	0.15	0.27	0.19
	lvbh	0.19	0.18	0.25	0.19	0.38	0.16	0.39	0.10
	rvbh	0.54	0.16	0.61	0.18	0.38	0.15	0.39	0.12
	avbh	0.09	0.12	0.13	0.12	0.28	0.10	0.20	0.16
	pvbh	0.25	0.12	0.16	0.14	0.43	0.09	0.43	0.11
vertebral canal	*vcb*	0.26	0.05	0.31	0.08	0.15	0.15	0.17	0.16
	vcl	0.26	0.14	0.33	0.16	0.28	0.09	0.67	0.18

Table 3. –Comparison of *intra-tester repeatability* and the *inter-tester reproducibility* of of MP_T implemented by *MBM* and *CBM*.

	dimensional parameter	*TRA*		*TER*	
		MM	*CBM*	*MM*	*CBM*
labial view	*CL*	0.18	0.11	0.21	0.08
	TL	0.08	0.08	0.05	0.04
	MD	0.13	0.10	0.13	0.06
	md	0.16	0.03	0.18	0.02
proximal view	*CC*	0.17	0.02	0.17	0.04
	Rmd	0.14	0.03	0.20	0.04
	Cbl	0.17	0.03	0.81	0.01
	Rbl	0.13	0.04	0.43	0.05
	md/MD	0.033	0.004	0.015	0.006